

# Pair-wise decoherence in coupled spin qubit networks

Andrea Morello<sup>1</sup>, P. C. E. Stamp<sup>1,2</sup>, and Igor S. Tupitsyn<sup>1,2,3</sup>

<sup>1</sup> *Department of Physics and Astronomy, University of British Columbia, Vancouver B.C. V6T 1Z1, Canada.*

<sup>2</sup> *Pacific Institute for Theoretical Physics, Vancouver B.C. V6T 1Z1, Canada.*

<sup>3</sup> *Russian Federal Research Center "Kurchatov Institute", Kurchatov Sq.1, Moscow 123182, Russia.*

Experiments involving phase coherent dynamics of networks of spins, such as echo experiments, will only work if decoherence can be suppressed. We show here, by analyzing the particular example of a crystalline network of  $\text{Fe}_8$  molecules, that most decoherence typically comes from pairwise interactions (particularly dipolar interactions) between the spins, which cause ‘correlated errors’. However at very low  $T$  these are strongly suppressed. These results have important implications for the design of quantum information processing systems using electronic spins.

PACS numbers: 03.65.Yz, 75.45.+j, 75.50.Xx

A worldwide effort is presently on to make nanoscale solid-state qubits, whose purity and reproducibility can easily be controlled. Microscopic spins, existing in molecular magnets [1], quantum dots [2] and semiconductors [3], or in doped fullerenes [4], are a leading candidate for this. In some of these systems (notably magnetic molecules), the individual qubit properties are controlled by chemistry instead of by nano-engineering (the ‘bottom-up’ approach [5]), with spin Hamiltonians and inter-molecular spin couplings known and controlled to at least 3 significant figures. Spin also possesses other advantages - information can be encoded in the topological spin phase, with no need to move electrons around. Using spins for quantum information will ultimately require (i) detecting and manipulating single-spins, and (ii) understanding and controlling decoherence.

Single spins have been detected in a few ingenious experiments [6], but we don’t yet have a general-purpose, single-spin detection/manipulation tool, analogous to single atom STM/AFM. Consider, however, an array of spins, each having a low-energy doublet of states whose splitting is easily controlled by a magnetic field. Even without addressing individual spins, one can still demonstrate coherent qubit operation, using external AC fields to promote resonant transitions between levels, and pulse sequences (e.g. spin echo) to manipulate the phase and measure decoherence rates. This approach is well known for room-temperature bulk NMR quantum computing [7]. Here we treat the case of electronic spins which, unlike nuclei, can be highly polarized at low  $T$ . We introduce a formalism allowing the description of any set of spin qubits obtained by truncation to low energy of a larger system, showing how the low- $T$  decoherence rate can be dramatically reduced, even for a network of mutually coupled qubits. To be specific, we treat the case where the qubit is obtained by taking an anisotropic high-spin nanomagnet [8] with easy axis  $\hat{z}$ , subject to a large transverse field  $\mathbf{H}_\perp$  (Fig. 1), giving a low-energy doublet of states with easily controllable energy separation,  $2\Delta_o(\mathbf{H}_\perp)$  [Fig. 2(a)]. To make quantitative and testable predictions, we then calculate the spin-echo decay rate in

a network of  $\text{Fe}_8$  molecules. This is a clean, crystalline and stoichiometric chemical compound [8, 9], where the inter-qubit and the qubit-environment interactions are known accurately, and it should be a good ‘benchmark’ for quantitative test of the theory.

(i) *Effective Hamiltonian:* In a transverse field  $\mathbf{H}_\perp$  the effective spin Hamiltonian of the  $\text{Fe}_8$  molecule, with total

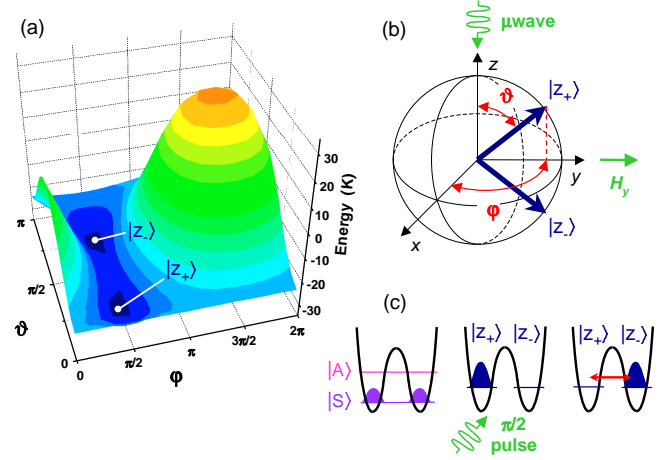


FIG. 1: (Color online) In a strong transverse field  $\mathbf{H}_\perp$ , the two potential wells of an easy axis spin system approach each other on the Bloch sphere. (a) The spin anisotropy energy for an  $\text{Fe}_8$  molecular spin with  $\mathbf{H}_\perp$  along  $\hat{y}$ , easy axis  $\hat{z}$  and hard axis  $\hat{x}$ , when  $\mu_o H_y = 2.5$  T. The low-lying states  $|z_\pm\rangle$ , are approximately localized in the two potential wells. The quantum-mechanical eigenstates are symmetric and antisymmetric superpositions of  $|z_\pm\rangle$  (see text), separated by the tunneling gap  $2\Delta_o$ . (b) The resonance experimental set-up and the spin states on the Bloch sphere; (c) At  $T \ll \Delta_o/k_B$  only the lowest-energy eigenstate is populated,  $|S\rangle = 2^{-1/2}(|z_+\rangle + |z_-\rangle)$ . A short  $\mu\text{wave}$  pulse prepares the system in the  $|z_+\rangle$  state ( $\pi/2$  rotation, corresponding to 1/4 of a Rabi oscillation). The spin then tunnels coherently between  $|z_+\rangle$  and  $|z_-\rangle$  at a frequency  $2\Delta_o/\hbar$ . The effect of static inhomogeneities in  $\Delta_o$  can be compensated by a  $\pi$ -pulse in a spin-echo sequence (not shown).

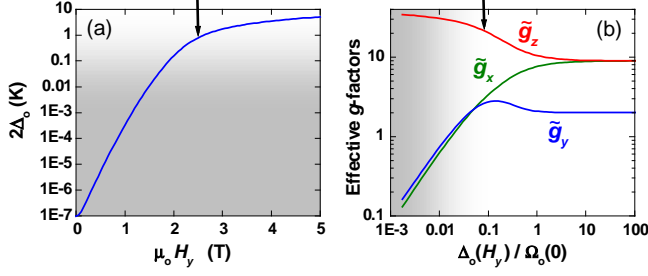


FIG. 2: (Color online) Fe<sub>8</sub> in a transverse field  $H_y$ : (a) Tunneling splitting  $2\Delta_0$  of the lowest doublet, as a function of  $H_y$ . (b) Effective  $g$ -factors for Fe<sub>8</sub> as a function of the ratio  $\Delta_0(H_y)/\Omega_0$ . In both figures, the values at  $\mu_0 H_y = 2.5$  T are indicated by a black arrow. Our decoherence rate calculations are valid when  $\Delta_0 \gg U_d$ , and do not apply in the grey areas shown.

spin  $S = 10$ , is controlled by crystal and external fields:

$$\mathcal{H}(\mathbf{S}) = -DS_z^2 + ES_x^2 + K_4^\perp(S_+^4 + S_-^4) - \gamma \mathbf{S} \cdot \mathbf{H}_\perp, \quad (1)$$

The easy/hard axes are along  $\hat{z}$  and  $\hat{x}$  respectively; here  $D/k_B = 0.23$  K,  $E/k_B = 0.094$  K,  $K_4^\perp/k_B = -3.28 \times 10^{-5}$  K,  $\gamma = g_e \mu_B \mu_0$  and  $g_e \approx 2$  is the isotropic  $g$ -factor of the spin-10 moment [10]. Henceforth we orient the external field along  $\hat{y}$ , ie.,  $\mathbf{H}_\perp \rightarrow \mathbf{H}_y$ ; this can tune the tunneling splitting  $2\Delta_0$  between the two lowest eigenstates over seven orders of magnitude [Fig. 2(a)]. Higher excited states are separated from the lowest doublet by a large gap  $\Omega_0 \approx 5$  K, and for  $k_B T \ll \Omega_0$  the giant spin can be truncated to an effective spin-1/2.

Given the two lowest doublet eigenstates,  $|\mathcal{S}(\mathbf{H}_\perp)\rangle$  and  $|\mathcal{A}(\mathbf{H}_\perp)\rangle$ , we write the quasi-localized states in the minima of the energy potential as  $|\mathcal{Z}_\pm\rangle = 2^{-1/2}(|\mathcal{S}\rangle \pm |\mathcal{A}\rangle)$  [Fig. 1(a)]. Defining the states  $|\mathcal{X}_\pm\rangle = 2^{-1/2}(|\mathcal{S}\rangle \pm i|\mathcal{A}\rangle)$ , we see that  $|\mathcal{X}_\pm\rangle$  and  $|\mathcal{Z}_\pm\rangle$  have the maximum (positive or negative) spin expectation values along  $\hat{x}$  or  $\hat{z}$  within the 2-dimensional subspace of the qubit, where  $|\mathcal{S}\rangle$  and  $|\mathcal{A}\rangle$  are the basis states. All of these Fe<sub>8</sub> spin states can be calculated by numerical diagonalization of (1). We then define qubit spin-1/2 operators  $\hat{s}_x, \hat{s}_y, \hat{s}_z$ , such that  $\hat{s}_z|\mathcal{S}\rangle = 1/2|\mathcal{S}\rangle$ , etc.

To describe the magnetic moment of the truncated spin qubit we introduce an effective  $g$ -tensor  $\tilde{\mathbf{g}}$ , also operating in the qubit subspace, and defined so that the qubit magnetic moment [11]  $m_\mu^s(\mathbf{H}) = \mu_B \sum_\nu \tilde{g}_{\mu\nu}(\mathbf{H}) s_\nu$ . In the geometry studied here, with  $\mathbf{H}$  along  $\hat{y}$ ,  $\tilde{\mathbf{g}}$  is diagonal, with components:

$$\tilde{g}_x = g_e(\langle \mathcal{X}_+ | S_x | \mathcal{X}_+ \rangle - \langle \mathcal{X}_- | S_x | \mathcal{X}_- \rangle); \quad (2a)$$

$$\tilde{g}_y = g_e(\langle \mathcal{S} | S_y | \mathcal{S} \rangle - \langle \mathcal{A} | S_y | \mathcal{A} \rangle); \quad (2b)$$

$$\tilde{g}_z = g_e(\langle \mathcal{Z}_+ | S_z | \mathcal{Z}_+ \rangle - \langle \mathcal{Z}_- | S_z | \mathcal{Z}_- \rangle). \quad (2c)$$

Numerical evaluation of  $\tilde{\mathbf{g}}$  shows it to be highly anisotropic and field-dependent [Fig. 2(b)].

Consider now two spin-10 Fe<sub>8</sub> molecules. The standard dipolar interaction  $\frac{1}{2} \sum_{i \neq j} \sum_{\mu, \nu} U_{\mu\nu}^{ij} S_\mu^i S_\nu^j$  has strength

$U_d = \mu_0 g_e^2 \mu_B^2 S^2 / 4\pi \mathcal{V}_c = 0.127$  K between nearest neighbors (here  $\mathcal{V}_c$  is the volume of the unit cell). However we are interested in the effective interaction between the *qubits* - this acquires a field-dependent and highly anisotropic tensor form  $\tilde{\mathbf{V}}^{ij}(\mathbf{H}_\perp) = \tilde{\mathbf{g}}^i \mathbf{U}^{ij} \tilde{\mathbf{g}}^j$  when written in the truncated qubit basis. There may also be exchange interactions [12] between the molecules - these however have never been observed in Fe<sub>8</sub>. Thus our low- $T$  Hamiltonian for the dipole-interacting molecules becomes:

$$H_{\text{eff}} = - \sum_i 2\Delta_0^i(\mathbf{H}_\perp) s_z^i + \frac{1}{2} \sum_{i \neq j} \sum_{\mu, \nu=x,y,z} \tilde{V}_{\mu\nu}^{ij}(\mathbf{H}_\perp) s_\mu^i s_\nu^j, \quad (3)$$

where the spins form a triclinic lattice [9], and we choose the qubit  $\hat{z}$  axis of quantization to be along the field (ie., along the original  $\hat{y}$  axis). The full Hamiltonian also includes local spin-phonon and hyperfine couplings, whose detailed form we will not need here.

(ii) *Decoherence*: Most general discussions of decoherence in qubit systems concentrate on ‘1-qubit’ decoherence, ie., that coming from the interactions of individual qubits with the environment [13, 14, 15]. In an insulating magnetic system like Fe<sub>8</sub> both nuclear spins and phonons will contribute to 1-qubit decoherence [16]. However this is not the only possible decoherence source. In a multi-qubit system one can have ‘correlated errors’, from pair-wise qubit interactions. A few analyses of this have been done [17]; depending on what model is chosen, these indicate that when qubits couple to the same bath, correlated decoherence is very serious, and may prevent error correcting codes from operating.

In the set-up imagined here, decoherence will show up in measurements of the dephasing time,  $T_2$ . We define the dimensionless decoherence rate as  $\gamma_\phi = \hbar/T_2\Delta_0$  (the ‘coherence Q-factor’ is then  $Q_\phi \sim \pi/\gamma_\phi$ ). We start by considering the role of dipolar interactions - these are important because they exist in all spin systems, and cause correlated errors via pair-wise spin interactions, exciting internal modes of the spin system (ie., no external environment). There are two ways to look at their contribution to  $\gamma_\phi$ . First, as a dephasing from dipole-mediated pair-flip processes, which in a resonance or echo experiment gives a homogenous absorption linewidth  $\langle \delta\omega_\phi \rangle = T_2^{-1}$ . Second, as a scattering of the uniform spin precession mode off thermal magnons. In what follows we will assume that  $U_d/2\Delta_0 \ll 1$ , ie., the dipolar interaction  $\ll$  the tunneling splitting - only then will dipolar decoherence be small enough to make an experiment worthwhile (in Fe<sub>8</sub> at, eg.,  $\mu_0 H_y = 2.5$  T we have  $U_d/2\Delta_0 \approx 0.16$ ). Since any reliable measurement of the decoherence rate will involve time-resolved spin-echo experiments, we neglect static inhomogeneous broadening in the calculations.

If  $U_d/2\Delta_0 \ll 1$  and  $k_B T \gtrsim \Delta_0$ , the contribution  $\gamma_\phi^{\text{V}}$  due to pair-flip processes can be expressed in terms of the second moment of the homogenous absorption line,

$\langle \delta\omega_\phi^2 \rangle \approx T_2^{-2}$ , by incorporating the  $\tilde{g}$ -factors in the van Vleck analysis [18]:

$$(\gamma_\phi^{\text{vV}})^2 \approx \left[ 1 - \tanh^2 \left( \frac{\Delta_o}{k_B T} \right) \right] \sum_{i \neq j} \left( \frac{\mathcal{A}_{yy}^{ij}}{\Delta_o} \right)^2, \quad (4a)$$

$$\mathcal{A}_{yy}^{ij} = \frac{U_d}{(2g_e S)^2} [(2\tilde{g}_y^2 + \tilde{g}_z^2) \mathcal{R}_{yy}^{ij} - (\tilde{g}_x^2 - \tilde{g}_z^2) \mathcal{R}_{xx}^{ij}], \quad (4b)$$

with  $\mathcal{R}_{\mu\nu}^{ij} = \mathcal{V}_c(|\mathbf{r}^{ij}|^2 \delta_{\mu\nu} - 3r_\mu^{ij} r_\nu^{ij})/|\mathbf{r}^{ij}|^5$ . The next term, neglected in Eq. (4a), is  $\sim O(U_d/\Delta_o)$ . This approach fails when  $k_B T \ll \Delta_o$ , since the line assumes a Lorentzian shape, where  $T_2$  is not related to  $\langle \delta\omega_\phi^2 \rangle$ .

Consider now magnon-mediated dipolar decoherence. In the experimental set-up we imagine here, a resonant tipping pulse applied to the spin ensemble causes a subsequent uniform spin precession (ie., coherent tunneling of the spins in the crystal between states  $|\mathcal{Z}_+\rangle$  and  $|\mathcal{Z}_-\rangle$ ). This is equivalent, in our effective spin language, to a magnon with wave vector  $\mathbf{q} = 0$ , with gapped energy  $\hbar\omega_o \sim 2\Delta_o$  when  $\Delta_o \gg U_d$ . However the dipolar interaction couples this magnon to other magnons [19]. The magnon spectrum  $\omega_{\mathbf{q}}$  is calculated using standard Holstein-Primakoff transformations [20] applied to Eq. (3). The lowest-order processes conserving both energy and momentum here are 4-magnon processes [cf. Fig. 3(b)]; for  $k_B T \ll U_d$  these are the only ones that contribute significantly (6-th and higher-order processes are  $\sim O(k_B T/U_d)^2$  relative to these). Selecting the  $T_2$  terms where the total spin polarization is unchanged, we derive a magnon contribution  $\gamma_\phi^m$  to  $\gamma_\phi$  given (again, for  $\Delta_o \gg U_d$ ) by:

$$\gamma_\phi^m = \frac{2\pi}{\hbar\Delta_o} \sum_{\mathbf{q}\mathbf{q}'} |\Gamma_{\mathbf{q}\mathbf{q}'}^{(4)}|^2 \mathcal{F}[\bar{n}_{\mathbf{q}}] \delta(\omega_o + \omega_{\mathbf{q}} - \omega_{\mathbf{q}'} - \omega_{\mathbf{q}-\mathbf{q}'}), \quad (5)$$

Here the relevant 4-magnon matrix element is  $\Gamma_{\mathbf{q}\mathbf{q}'}^{(4)} = (1/4N)[\mathcal{K}^{(4)}(\mathbf{q}, \mathbf{q}') + \mathcal{K}^{(4)}(\mathbf{0}, \mathbf{q}')]$ , where  $\mathcal{K}^{(4)}(\mathbf{q}, \mathbf{q}') = 2K_{yy}(\mathbf{q} - \mathbf{q}') - K_{zz}(\mathbf{q}) - K_{xx}(\mathbf{q})$  and

$$K_{\mu\nu}(\mathbf{q}) = U_d \frac{\tilde{g}_\mu \tilde{g}_\nu}{g_e^2 S^2} \sum_{l \in V} \mathcal{R}_{\mu\nu}^{ol} e^{i\mathbf{q} \cdot \mathbf{r}^l}. \quad (6)$$

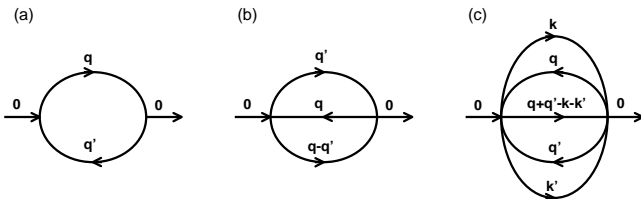


FIG. 3: Feynman self-energy graphs for the  $\mathbf{q} = \mathbf{0}$  uniform precession mode, interacting with magnon excitations. We depict (a) a 3-magnon process, which is ruled out by energy conservation, (b) a 4-magnon process, and (c) a 6-magnon process.

$\mathcal{F}[\bar{n}_{\mathbf{q}}]$  is the usual Bose statistical weighting of the magnon thermal occupation numbers  $\bar{n}_{\mathbf{q}}$ , and  $\hbar\omega_{\mathbf{q}} = (A_{\mathbf{q}}^2 - 4|B_{\mathbf{q}}|^2)^{1/2}$  with  $A_{\mathbf{q}} = 2\Delta_o - \frac{1}{4}[2K_{yy}(0) - K_{zz}(\mathbf{q}) - K_{xx}(\mathbf{q})]$  and  $B_{\mathbf{q}} = \frac{1}{8}[K_{zz}(\mathbf{q}) - K_{xx}(\mathbf{q}) - 2iK_{xz}(\mathbf{q})]$  for any  $\mathbf{q}$ . The magnon analysis requires spin polarization close to unity, ie.,  $k_B T < 2\Delta_o$ , and therefore complements the ‘van Vleck’ approach from the low- $T$  side. It’s interesting to notice that the two methods yield different  $T$ -dependencies,  $\sim \exp(-\Delta_o/k_B T)$  for  $\gamma_\phi^{\text{vV}}$  and  $\sim \exp(-2\Delta_o/k_B T)$  for  $\gamma_\phi^m$ . The crossover occurs around  $k_B T \sim \Delta_o$ , where the lineshape turns from Gaussian ( $k_B T > \Delta_o$ ) to Lorentzian ( $k_B T < \Delta_o$ ). Full quantitative details will appear in a long paper [21].

To these 2-qubit decoherence processes one must also add 1-qubit decoherence processes to find the total  $\gamma_\phi$  that would be measured in an experiment. The contributions from interaction with phonons and nuclear spins have been calculated for Fe<sub>8</sub> elsewhere [16]. In large transverse fields nuclear spins give a rate  $\gamma_\phi^{\text{NS}} = E_o^2/2\Delta_o^2$ , where  $E_o$  is the half-width of the Gaussian multiplet of nuclear-spin states coupled to the qubit. The phonon decoherence rate is given for Fe<sub>8</sub> by [22]:

$$\gamma_\phi^{\text{ph}} = \frac{\mathcal{M}_{AS}^2 \Delta_o^2}{\pi \rho c_s^5 \hbar^3} \coth \left( \frac{\Delta_o}{k_B T} \right), \quad (7)$$

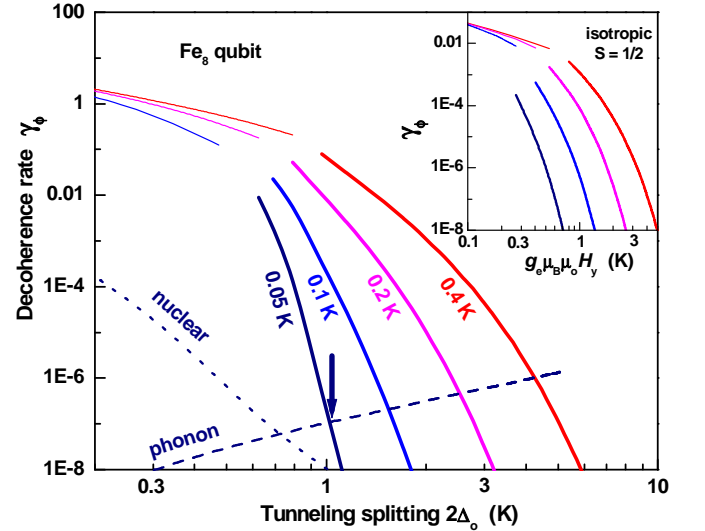


FIG. 4: (Color online) Dimensionless decoherence rates  $\gamma_\phi = \hbar/T_2 \Delta_o$  as a function of tunneling gap  $2\Delta_o$  in Fe<sub>8</sub>, at the indicated  $T$ . Thin lines:  $\gamma_\phi^{\text{vV}}$  arising from pair-flip processes, Eq. (4a). We omit  $\gamma_\phi^{\text{vV}}$  at  $T = 0.05 \text{ K} \ll U_d/k_B$ . Thick lines:  $\gamma_\phi^m$  from magnon scattering, Eq. (5). The gap between the  $\gamma_\phi^{\text{vV}}$  and  $\gamma_\phi^m$  lines is the crossover region between the validity of the two methods. The dashed and dotted lines show respectively the phonon [ $\gamma_\phi^{\text{ph}}$ , Eq. (7)] and nuclear ( $\gamma_\phi^{\text{NS}}$ ) decoherence rates at  $T = 0.05 \text{ K}$ . The arrow indicates the optimal operation point of the Fe<sub>8</sub> spin qubit at  $T = 0.05 \text{ K}$ . Inset:  $\gamma_\phi^{\text{vV}}$  and  $\gamma_\phi^m$  for an isotropic spin-1/2 on the same Fe<sub>8</sub> lattice, as a function of the Zeeman gap  $g_e \mu_B \mu_o H_y$ .

where  $\mathcal{M}_{AS}^2(H_y) \approx \frac{4}{3}D^2|\langle A|S_yS_z + S_zS_y|S\rangle|^2$ , with density  $\rho = 1920 \text{ kg/m}^3$  and sound velocity  $c_s = 1386 \text{ m/s}$ .

Fig. 4 summarizes the results of all these calculations. Except at very low  $T$  and large  $\Delta_o$ , dipolar decoherence completely dominates over nuclear and phonon decoherence. The optimal operating point at  $T = 0.05 \text{ K}$ , having minimum total decoherence, is found where  $2\Delta_o \approx 1 \text{ K} \approx 20 \text{ GHz}$ , at  $\mu_o H_y \approx 2.6 \text{ T}$ ; here the decoherence quality factor is  $Q_\phi \sim 10^7$ , with a coherence time  $T_2 \sim 1 \text{ ms}$ . Since  $\gamma_\phi^{\text{ph}} \propto \coth(\Delta_o/k_B T)$  is essentially  $T$ -independent in this regime, while dipolar contributions to  $\gamma_\phi$  still vary strongly, a further decrease in temperature would not substantially decrease  $\gamma_\phi$ , but would allow operation at lower frequencies. It is instructive to compare the results for the  $\text{Fe}_8$  qubit, with the case of a fictitious isotropic spin-1/2 on the same lattice (inset Fig. 4), obtained by setting  $\tilde{g}_x = \tilde{g}_y = \tilde{g}_z = g_e$  and replacing  $2\Delta_o$  by  $g_e\mu_B\mu_o H_y$  in all our formulas. We then deal with simple Larmor precession instead of spin tunneling. There is a clear reduction in  $\gamma_\phi$ , but no trivial proportionality factor, because of the strong variation of  $\tilde{g}_\mu(H_y)$  in the  $\text{Fe}_8$  qubit [Fig. 2(b)].

We now consider the more general implications of these results. Note first that even for the set-up considered here, correlated errors cause large decoherence - we suspect they will even more strongly affect higher-order entanglement between the qubits. This is in line with the results in the quantum information literature [17], but the concrete calculation here reveals a surprising feature, viz., that at very low  $T$ , the contribution of correlated errors can be made much *smaller* than the single-qubit errors coming from hyperfine and spin-phonon couplings.

Dipolar interactions are dangerous for spin qubit design, but they are hard to screen. One way to reduce their effects (apart from going to very low  $T$  [23]) would be to go to lower dimensional spin networks; recent progress in attaching and assembling nanomagnets on surfaces [24], or even in chain structures [25] might then yield viable architectures. Designs in which dipolar inter-qubit couplings can be made small - eg., low-spin systems like  $\text{V}_{15}$  or  $\text{Cr}_7\text{Ni}$  [26] - and where the inter-qubit couplings responsible for information manipulation can be switched on and off, are clearly favored.

We believe that we have captured the intrinsic decoherence processes in networks of coupled spin qubits, extending to the case where the qubit is the low-energy truncation of a larger system. Spin-echo experiments on well-characterized systems like  $\text{Fe}_8$  would give a stringent test of the theory. Perhaps more important, such experiments would allow exploration of different spin network architectures, even before the manipulation of individual spins in such networks becomes possible.

We thank A. Burin, W. N. Hardy, A. Hines, A. J. Leggett, and G. A. Sawatzky for stimulating discussions, and NSERC and PITP for support.

- 
- [1] F. Troiani *et al.*, Phys. Rev. Lett. **94**, 190501 (2005).
  - [2] D. Loss and D. P. DiVincenzo, Phys. Rev. A. **57**, 120 (1998).
  - [3] B. E. Kane, Nature **393**, 133 (1998); A. M. Stoneham, A. J. Fisher, and P. T. J. Greenland, J. Phys.: Condens. Matter **15**, L447 (2003).
  - [4] J. J. L. Morton *et al.*, Nat. Phys. **2**, 40 (2006).
  - [5] C. Joachim, J. K. Gimzewski, and A. Aviram, Nature **408**, 541 (2000).
  - [6] D. Rugar *et al.*, Nature **430**, 329 (2004); J. M. Elzerman *et al.*, Nature **430**, 431 (2004).
  - [7] N. A. Gershenfeld and I. L. Chuang, Science **275**, 350 (1997); L. M. K. Vandersypen *et al.*, Nature **414**, 883 (2001).
  - [8] D. Gatteschi, A. Caneschi, L. Pardi, and R. Sessoli, Science **265**, 1054 (1994).
  - [9] K. Wieghardt *et al.* Angew. Chem. Int. Ed. Engl. **23**, 77 (1984).
  - [10] I. S. Tupitsyn and B. Barbara, *Magnetism: molecules to materials, vol III, 109-168* Ch. 9, eds. Miller, J. S. & Drillon, M. (Wiley-VCH, Weinheim, 2002); see also S. Carretta *et al.*, Phys. Rev. Lett. **92**, 207205 (2004).
  - [11] We drop a term  $m^S(\mathbf{H}_\perp) = g_e\mu_B(\langle S|S_y|S\rangle + \langle A|S_y|A\rangle)/2$  from the moment, since it contributes only to the static demagnetisation field.
  - [12] W. Wernsdorfer, N. Aliaga-Alcalde, D. N. Hendrickson, and G. Christou, Nature **416**, 406 (2002).
  - [13] A. J. Leggett *et al.*, Rev. Mod. Phys. **59**, 1 (1987).
  - [14] U. Weiss, *Quantum dissipative systems* (World Scientific, Singapore, 1999).
  - [15] N. V. Prokof'ev and P. C. E. Stamp, Rep. Prog. Phys. **63**, 669 (2000).
  - [16] P. C. E. Stamp and I. S. Tupitsyn, Phys. Rev. B **69**, 014401 (2004).
  - [17] R. Alicki, *et al.*, Phys. Rev. A **65**, 062101 (2002); B. M. Terhal and G. Burkard, Phys. Rev. A **71**, 012336 (2005); R. Klesse and S. Frank, Phys. Rev. Lett. **95**, 230503 (2005); E. Novais and H. U. Baranger, Phys. Rev. Lett. **97**, 040501 (2006).
  - [18] J. H. van Vleck, Phys. Rev. **74**, 1168 (1948); M. McMillan and W. Opechowski, Can. J. Phys. **38**, 1168 (1960).
  - [19] P. Pincus, M. Sparks, and R. C. LeCraw, Phys. Rev. **124**, 1015 (1961).
  - [20] T. Holstein and H. Primakoff, Phys. Rev. **58**, 1098 (1940).
  - [21] A. Morello, P. C. E. Stamp, and I. S. Tupitsyn, in preparation.
  - [22] This expression corrects Eq. (9) of [16], from which a factor  $\sim \Delta_o^2/\Omega_o^2$  was accidentally omitted.
  - [23] Note, however, that even at low *lattice*  $T$ , pair-flip decoherence will be large if the spin system is not in a thermal state (eg., in the middle of a computation).
  - [24] M. Cavallini *et al.*, Nano Letters **3**, 1527 (2003); L. Zobbi *et al.*, Chem. Comm., 1640 (2005).
  - [25] R. Clérac, H. Miyasaka, M. Yamashita, and C. Coulon, J. Am. Chem. Soc. **124**, 12837 (2002).
  - [26] I. Chiorescu *et al.*, Phys. Rev. Lett. **85**, 4807 (2000); F. Troiani *et al.*, Phys. Rev. Lett. **94**, 207208 (2005).